Appl. Chem. Eng., Vol. 30, No. 3, June 2019, 379-383
https://doi.org/10.14478/ace.2019.1029

Article

Thiolated Protein A-functionalized Bimetallic Surface Plasmon Resonance Chip for Enhanced Determination of Amyloid Beta 42

Hyung Jin Kim, Chang-Duk Kim*, and Young-Soo Sohn†

Department of Biomedical Engineering, Daegu Catholic University, Gyeongsan-si, Gyeongbuk 38430, Republic of Korea
**Department of Physics, Kyungpook National University, Daegu 41566, Republic of Korea*
(Received April 22, 2019; Revised May 8, 2019; Accepted May 16, 2019)

Abstract

The capability of detecting amyloid beta 42 (Aβ42), a biomarker of Alzheimer's disease, using a thiolated protein A-functionalized bimetallic surface plasmon resonance (SPR) chip was investigated. An optimized configuration of a bimetallic chip containing gold and silver was obtained through calculations in the intensity measurement mode. The surface of the SPR bimetallic chip was functionalized with thiolated protein A for the immobilization of Aβ42 antibody. The response of the thiolated protein A-functionalized bimetallic chip to Aβ42 in the concentration range of 50 to 1,000 pg/mL was linear. Compared to protein A without thiolation, the thiolated protein A resulted in greater sensitivity. Therefore, the thiolated protein A-functionalized bimetallic SPR chip can be used to detect very low concentrations of the biomarker for Alzheimer's disease.

***Keywords**: Surface plasmon resonance, Amyloid beta 42, Alzheimer's disease, Intensity measurement*

1. Introduction

Globally, approximately 50 million people have dementia, and nearly 10 million people develop dementia with age every year[1]. Dementia refers to a decline in cognitive function, which interferes with daily living by affecting memory, thinking, judgment, behavior, and so forth. Types of dementia include Alzheimer's disease (AD), Parkinson's disease, dementia with Lewy bodies, and frontotemporal dementia[2-8]. The most common type of dementia is AD, a neurodegenerative dementia. Amyloid beta 42 (Aβ42), total tau, and phosphorylated tau in the cerebrospinal fluid (CSF) are the most widely known biomarkers of AD[3]. Among these markers, interest in Aβ42 is increasing since it was reported that using an AD mouse model, the Aβ42 level in CSF is directly correlated with that in plasma[9]. However, further investigations into quantification of the Aβ42 levels in the blood are required to diagnose AD[9,10]. Aβ42 is produced by cleavage of the amyloid precursor protein. The peptide precipitates in the form of plaque in the brain and regresses the nerves responsible for memory and cognition. The deposition of Aβ42 is known to begin 10 years before the onset of Alzheimer's symptoms[4,5]. Since Aβ42 accumulates in the brain, Alzheimer's patients have less than 500 pg/mL of Aβ42 in their CSF[3]. A method of curing AD has not been found to date. Therefore, early diagnosis of AD would open the window for the development of medicine as well as a cure. Enzyme-linked immunosorbent assays have been widely used as a technique to detect Aβ[9,11,12]. However, interesting research efforts have been made to develop label-free detection techniques based on electrical and optical methods[13-16].

Recently, much attention has been paid to surface plasmon resonance (SPR) sensors, which can monitor biomolecular interactions with highly sensitive, label-free, and real-time detection[17-19]. Four different SPR detection modes, namely, angular interrogation, phase interrogation, intensity measurement, and wavelength measurement are available[20]. Angular interrogation and intensity measurement modes utilize the SPR reflectance curve, a graph of the intensity of the reflected light with respect to the incident angle. The reflectance curve relies on the optical properties of the SPR sensor components and system. The angle at which the reflected light is minimum on the reflectance curve is called the resonance angle. Changes in the refractive index of the medium causes a shift in the reflectance curve. Measurements in the angular interrogation mode monitor the resonance angle according to changes in the refractive index of the medium, whereas the intensity measurement mode monitors the reflectance at a fixed angle at the maximum tangential slope point on the reflectance curve[21,22]. To enhance the resolution in the angular interrogation mode, the optical path should be lengthened. This requirement may limit the compactness of an SPR sensor system with high resolution. Modifying the SPR sensor chip and applying another detection mode is an alternative approach to enhance the resolution of the sensor system. The material conventionally used for SPR chips is gold (Au) due to biocompatibility. However, it limits the detection of trace-level concentration of biomolecules[23]. Silver (Ag) is also a good candidate for SPR chips, and its reflectance curve has a narrower linewidth and sharper dip, leading to a higher

† Corresponding Author: Daegu Catholic University,
Department of Biomedical Engineering, Gyeongsan-si, Gyeongbuk 38430, Republic of Korea
Tel: +82-53-850-2513 e-mail: sohnys@cu.ac.kr

pISSN: 1225-0112 eISSN: 2288-4505

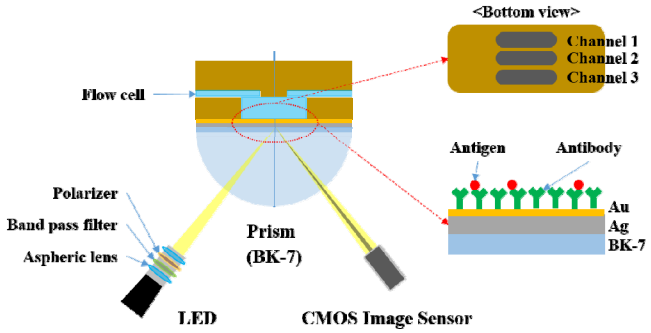

Figure 1. Schematic diagram of the SPR sensor system with the bimetallic chip configuration.

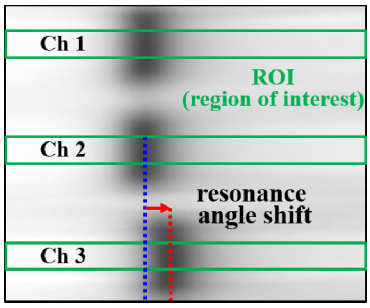

Figure 2. The reflected light acquired by the 2D-CMOS image sensor for three channels. The intensity of the reflected light in ROI was converted into a reflectance curve.

tangential slope. Intensity measurement mode can take advantage of the higher tangential slope of the reflectance curve. However, since Ag is easily oxidized, it cannot be used alone[21]. Thus, bimetallic chips containing Ag and Au with the advantages of both materials have become attractive options for intensity measurements[21,22,24-26].

Antibodies have two domains: the Fc (fragment crystallizable) domain and the Fab (fragment antigen binding) domain. The antigen reacts only with the Fab domain of the antibody. Protein A and protein G are well-known antibody-binding proteins[27]. Compared to protein G, which has three domains, protein A has five domains at the amino terminus; these domains bind specifically to the Fc domain of the antibody[27,28]. To increase the probability of antigen-antibody binding, it is preferable for the antigen-binding sites (Fab domain) of the antibody to face towards the sample containing the antigen. It is also well known that there is a high affinity between thiol groups and the Au surface. Thus, a thiolated antibody-binding protein is profitable for optimized antibody immobilization[27].

In this study, a thiolated protein A-functionalized bimetallic SPR chip was developed to detect very low concentrations of Aβ42 to aid AD diagnosis. To achieve higher resolution with a bimetallic chip containing Ag, we utilized the intensity measurement mode. The optimized bimetallic chip configuration used for this detection mode was evaluated. The bimetallic SPR chip was functionalized with thiolated protein A and the antibody of Aβ42 (anti-Aβ42) for the detection of Aβ42. The SPR response of the thiolated protein A-functionalized bimetallic chip to very low concentrations of Aβ42 including the critical concentration was analyzed. To confirm the effect of the thiolated protein A, the results were compared to those obtained using protein A without thiolation.

2. Materials and Methods

The SPR sensor system was based on the Kretschman configuration. The light source for the system was a light-emitting diode (LED) with a peak wavelength of 770 nm (OpNext Inc., Japan), which was p-polarized using a polarizer. The bandwidth of the wavelength was reduced using a band pass filter (770 ± 5 nm). The p-polarized light in the form of a wedge beam with an angle range of 7.14° reached the sensor chip after passing through a prism (BK7, cylindrical). The reflected light from the sensor chip was acquired by a 2-dimensional complementary-metal-oxide-semiconductor (2D-CMOS: 1,280 × 1,024 pixels, IDS Co., Germany) image sensor. Figure 1 shows the schematic diagram of the SPR sensor system with the bimetallic chip configuration. Figure 2 shows the image acquired by the 2D-CMOS and the resonances (black dark area) that occurred in three channels. The region of interest (ROI) was set from the acquired image, and the intensity of the reflected light was converted into a reflectance curve. In Figure 2, the bottom channel shows the shift of the resonance, implying that there was a difference in the refractive index near the metal surface between channel 3 and channels 1 or 2. In fabricating the SPR chip, a very thin chromium (Cr) layer was used as an adhesion layer. After the deposition of Cr, Ag and Au layers were sequentially deposited with an e-beam evaporator.

Thiolated protein A was prepared through the reaction of 150 μL of protein A at a concentration of 200 μg/mL with 3.44 mg of 2-iminothiolane at 4 ℃ for 30 minutes. After the reaction, excess 2-iminothiolane was removed with a desalting column through centrifugation at 1,000 rpm for 3 minutes at 4 ℃. To enhance coupling efficiency between the thiolated protein A and anti-Aβ42, 4 μg/mL of 1-ethyl-3-(3-dimethylamino-propyl) carbodiimide (EDC) (1.5 μL) and 11 μg/mL of N -hydroxysulfosuccinimide (Sulfo - NHS) (1.5 μL) were utilized since sulfo-NHS/EDC activate the carboxyl groups to react with primary amine unit to form amide crosslinks.

Next, 200 μg/mL of thiolated protein A, 150 μg/mL of anti-Aβ42, 100 μg/mL of bovine serum albumin (BSA), and various concentrations of Aβ42 were sequentially injected into the flow cell of the SPR sensor system. BSA was used to block non-specific bindings, and all proteins were diluted in phosphate buffered saline (PBS) solution. All sample solutions were injected at a constant flow rate of 10 μL/min using a peristaltic pump, and air bubbles were removed using a degreaser before injection of the samples into the SPR sensor system. All experimental temperatures were maintained at 25 ℃. Protein A, 2-iminothiolane, PBS, and BSA were purchased from Sigma Aldrich (MO, USA). EDC and Sulfo-NHS were purchased from Thermo Scientific (IL, USA). Aβ42 and anti-Aβ42 were purchased from Merck Millipore (Darmstadt, Germany).

Table 1. Theoretical Calculation of the Characteristics of the Bimetallic Chips with Different Thickness Values and the Conventional Au chip. △R Stands for the Reflectance Change due to Changes in the Refractive Index from 1.335 to 1.337

Configuration	Linewidth [degree, °]	Maximum slope [%/degree, %/°] at incident angle (θ_m[°])	ΔR [%] (R (n = 1.337) - R (n = 1.335)) at θ_m
Au (50 nm)	1.50	99 (θ_m = 66.63°)	19.38
Au (30 nm)/Ag (20 nm)	1.26	115 (θ_m = 66.78°)	22.69
Au (25 nm)/Ag (25 nm)	1.18	122 (θ_m = 66.73°)	23.86
Au (20 nm)/Ag (30 nm)	1.08	131.5 (θ_m = 66.64°)	25.09
Au (15 nm)/Ag (35 nm)	0.96	146.5 (θ_m = 66.53°)	27.64
Au (10 nm)/Ag (40 nm)	0.82	170 (θ_m = 66.35°)	30.73

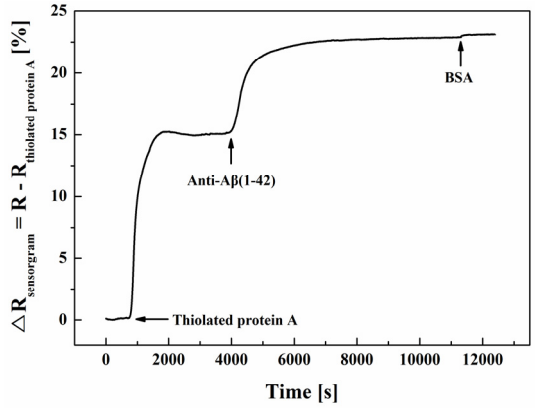

Figure 3. Sensorgram of the bimetallic SPR chip with sequential injection of thiolated-protein A, anti-Aβ42, and BSA.

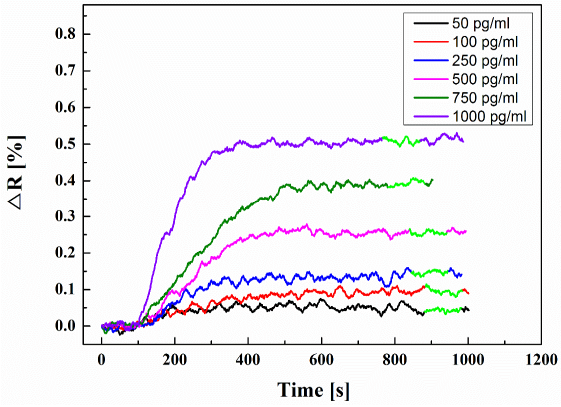

Figure 4. Responses of the functionalized chip to various concentrations of Aβ42.

3. Results and Discussions

Table 1 lists the results for various configurations of the bimetallic chips through Fresnel reflectivity calculation. In Table 1, the refractive index of the reference sample medium for this calculation was set to 1.335, which is quite close to the refractive index of the PBS solution. The refractive indexes of Ag and Au are n_{Ag} = 0.032151 + i5.3463 and n_{Au} = 0.14430 + i4.6583, respectively[29]. The refractive index of BK7 is n_{BK7} = 1.511. As the amount of Ag in the bimetallic chip increased, the linewidth of the reflectance curve tended to become narrower. Among the various configurations of the bimetallic chips listed in Table 1, the Ag (40 nm)/Au (10 nm) chip exhibited the narrowest linewidth, resulting in the greatest slope value. The larger the slope value, the steeper the reflectance curve become. This means that the variation of the reflectance due to refractive index change at the angle where the slope is the steepest would become the largest. △R in Table 1 stands for the amount of the change in reflectance at a fixed incident angle due to changes in the refractive index from n = 1.335 to n = 1.337, where R is the reflectance on the reflectance curve at a fixed incident angle. The calculation demonstrated that the Ag (40 nm)/Au (10 nm) chip showed the largest variation of reflectance with the same refractive index change. Therefore, the Ag (40 nm)/Au (10 nm) chip was selected for this study.

Figure 3 shows a sensorgram representing the response of the bimetallic SPR chip to sequential injection of thiolated protein A, anti-Aβ42, and BSA. The vertical axis of this sensorgram is the difference in reflectance since the intensity measurement mode was utilized in this study. $\triangle R_{sensorgram}$ is the subtraction of reflectance of the functionalized thiolated protein A at the incident angle of the steepest slope ($R_{thiolated\ protein\ A}$) from the reflectance of sequential injections of proteins at the same incident angle (R). The amount of change sufficiently demonstrated that all the proteins were immobilized on the bimetallic chip surface. Aβ42 at concentrations of 50, 100, 250, 500, 750, and 1,000 pg/mL was injected into the SPR system after functionalization of the bimetallic chip with thiolated protein A, anti-Aβ42, and BSA. Figure 4 shows the SPR response of the functionalized bimetallic chip to six different concentrations of Aβ42 in the intensity measurement mode. The measurement for the changes in reflectance were carried out at a fixed incident angle of 65.26°. After the response reached a stable phase, the output response to each concentration was obtained by averaging over a 100-second period of the signal in the plateau. As expected, △R increased with the Aβ42 concentration. Each experiment was performed three times, and the average responses to 50, 100, 250, 500, 750, and 1,000 pg/mL of Aβ42 for three replicates were 0.04292, 0.09762, 0.15161, 0.2662, 0.39682, and 0.50627%, respectively. From the linear regression shown in Figure 5, the sensitivity (the slope of the regression line) was 0.000474% · mL/pg, and the correlation coefficient was 0.998, showing good linearity. The error bars represent the standard deviation for three replicates. △R in Figures 4 and 5 represents the difference in reflectance at the specified incident angle be-

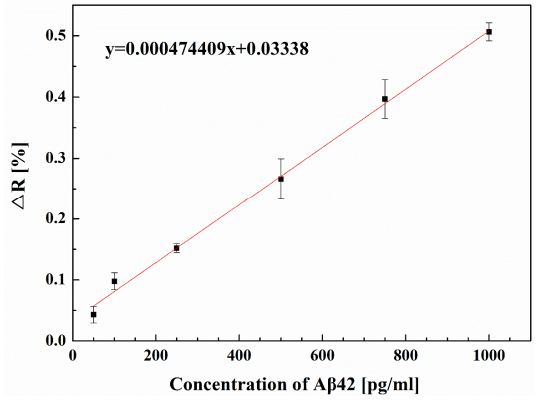

Figure 5. Regression line of average responses to Aβ42 concentrations from 50 pg/mL to 1,000 pg/mL. Error bar stands for standard deviation of three replicates.

fore and after the change in refractive index by protein injections. These results confirm that the thiolated protein A-functionalized bimetallic SPR chip could detect a critical concentration of Aβ42 in the intensity measurement mode.

To validate the efficiency of thiolated protein A in detecting Aβ42, characteristics of the bimetallic chips functionalized by protein A with and without thiolation were compared. The sensitivity was improved with thiolation since the sensitivity of the chip functionalized without thiolation was 0.000288% · mL/pg[25]. The limit of detection (LOD), known as the lowest concentration of analyte that can be reliably distinguished in a sample, was calculated using Eq. (1)[30,31].

$$\mathrm{LOD} = \frac{3\sigma}{s} \quad (1)$$

where σ is the standard deviation of the blank, and s is the slope of the regression line. The standard deviation of the blank was 0.006187%. Thus, the LOD was 39.12 pg/mL, which is lower than 54.57 pg/mL obtained from the chip functionalized by protein A without thiolation[25]. From these experiments, the use of thiolated protein A with a bimetallic SPR chip containing a higher amount of Ag enhanced sensitivity in the intensity measurement mode.

4. Conclusions

The characteristics of the bimetallic SPR chip functionalized by thiolated protein A were investigated for the detection of trace-level concentrations of Aβ42 in the intensity measurement mode. The results suggested that a higher Ag ratio resulted in a narrower linewidth, which was advantageous for intensity measurements. The SPR response of the thiolated protein A-functionalized bimetallic chip to very low Aβ42 concentration levels was linear. Compared to protein A without thiolation, the thiolated protein A showed enhanced sensitivity and lower LOD. Therefore, the results confirmed the capability of the thiolated protein A-functionalized bimetallic SPR chip to detect low concentrations of biomarkers in the clinical field.

References

1. World Health Organization, Dementia, Key facts, http://www.who.int/news-room/fact-sheets/detail/dementia, Accessed in January (2019).
2. S. A. Gale, D. Acar, and K. R. Daffner, Dementia, *Am. J. Med.*, **131**, 1161-1169 (2018).
3. C. Humpel, Identifying and validating biomarkers for Alzheimer's disease, *Trends Biotechnol.*, **29**, 26-32 (2011).
4. R. J. Perrin, A. M. Fagan, and D. M. Holtzman, Multi-modal techniques for diagnosis and prognosis of Alzheimer' disease, *Nature*, **461**, 916-922 (2009).
5. K. Blennow, B. Dubois, A. M. Fagan, P. Lewczuk, M. J. de Leon, and H. Hampel, Clinical utility of cerebrospinal fluid biomarkers in the diagnosis of early Alzheimer's disease, *Alzheimers Dement.*, **11**, 58-69 (2015).
6. S. G. Reich and J. M. Savitt, Parkinson disease, *Med. Clin. North Am.*, **103**, 337-350 (2019).
7. A. M. Sanford, Lewy body dementia, *Clin. Geriatr. Med.*, **34**, 603-615 (2018).
8. M. Bruuna, J. Koikkalainen, H. F. M. Rhodius-Meester, M. Baroni, L. Gjerum, M. van Gils, H. Soininen, A. M. Remes, P. Hartikainen, G. Waldemar, P. Mecocci, F. Barkhof, Y. Pijnenburg, W. M. van der Flier, S. G. Hasselbalch, J. Lötjönen, and K. S. Frederiksen, Detecting frontotemporal dementia syndromes using MRI biomarkers, *Neuroimage Clin.*, **22**, 101711 (2019).
9. S. M. Cho, H. V. Kim, S. Lee, H. Y. Kim, W. Kim, T. S. Kim, D. J. Kim, and Y. S. Kim, Correlations of amyloid-β concentrations between CSF and plasma in acute Alzheimer mouse model, *Sci. Rep.*, **4**, 6777 (2014).
10. T. Kasai, T. Tokuda, M. Taylor, M. Kondo, D. M. A. Mann, P. G. Foulds, M. Nakagawa, and D. Allsop, Correlation of Aβ oligomer levels in matched cerebrospinal fluid and serum samples, *Neurosci. Lett.*, **551**, 17-22 (2013).
11. L. Janssen, F. Sobott, P. P. D. Deyn, and D. V. Dam, Signal loss due to oligomerization in ELISA analysis of amyloid-beta can be recovered by a novel sample pre-treatment method, *MethodsX*, **2**, 112-123 (2015).
12. A. C. Klaver, L. M. Patrias, J. M. Finke, and D. A. Loeffler, Specificity and sensitivity of the Abeta oligomer ELISA, *J. Neurosci. Methods*, **195**, 249-254 (2011).
13. Y. K. Yoo, J. Kim, G. Kim, Y. S. Kim, H. Y. Kim, S. Lee, W. W. Cho, S. Kim, S.-M. Lee, B. C. Lee, J. H. Lee, and K. S. Hwang, A highly sensitive plasma-based amyloid-β detection system through medium-changing and noise cancellation system for early diagnosis of the Alzheimer's disease, *Sci. Rep.*, **7**, 8882 (2017).
14. F. S. Diba, S. Kim, and H. J. Lee, Electrochemical immunoassay for amyloid-beta 1-42 peptide in biological fluids interfacing with a gold nanoparticle modified carbon surface, *Catal. Today*, **295**, 41-47 (2017).
15. N. Xia, L. Liu, M. G. Harrington, J. Wang, and F. Zhou, Regenerable and simultaneous SPR detection of Aβ(1-40) and Aβ(1-42) peptides in cerebrospinal fluids with signal amplification by streptavidin conjugated to an N-terminus-specific antibody, *Anal. Chem.*, **82**, 10151-10157 (2010).
16. I.-H. Chou, M. Benford, H. T. Beier, G. L. Coté, M. Wang, N. Jing, J. Kameoka, and T. A. Good, Nanofluidic biosensing for β

-amyloid detection using surface enhanced raman spectroscopy (SERS), *Nano Lett.*, **8**, 1729-1735 (2008).
17. J. Homola, S. S. Yee, and G. Gauglitz, Surface plasmon resonance sensors: Review, *Sens. Actuators B*, **54**, 3-15 (1999).
18. H. Šípová and J. Homola, Surface plasmon resonance sensing of nucleic acids: A review, *Anal. Chim. Acta*, **773**, 9-23 (2013).
19. T.-F. Ma, Y.-P. Chen, J.-S. Guo, and W. Wang, Cellular analysis and detection using surface plasmon resonance imaging, *Trends Analyt. Chem.*, **103**, 102-109 (2018).
20. F.-C. Chien and S.-J. Chen, A sensitivity comparison of optical biosensors based on four different surface plasmon resonance modes, *Biosens. Bioelectron.*, **20**, 633-642 (2004).
21. Y. K. Lee, Y.-S. Sohn, K.-S. Lee, W. M. Kim, and J.-O. Lim, Waveguide-coupled bimetallic film for enhancing the sensitivity of a surface plasmon resonance sensor in a fixed-angle mode, *J. Korean Phys. Soc.*, **62**, 475-480 (2013).
22. K.-S. Lee, T. S. Lee, I. Kim, and W. M. Kim, Parametric study on the bimetallic waveguide coupled surface plasmon resonance sensors in comparison with other configurations, *J. Phys. D*, **46**, 125302 (2013).
23. X. C. Yuan, B. H. Ong, Y. G. Tan, D. W. Zhang, R. Irawan, and S. C. Tjin, Sensitivity-stability optimized surface plasmon resonance sensing with double metal layers, *J. Opt. A*, **8**, 959-963 (2006).
24. H.-S. Lee, T.-Y. Seong, W. M. Kim, I. Kim, G.-W. Hwang, W. S. Lee, and K.-S. Lee, Enhanced resolution of a surface plasmon resonance sensor detecting C-reactive protein via a bimetallic waveguide-coupled mode approach, *Sens. Actuators. B*, **266**, 311-317 (2018).
25. H. J. Kim, Y.-S. Sohn, C.-D. Kim, and D.-H. Jang, Surface plasmon resonance sensing of a biomarker of alzheimer disease in an intensity measurement mode with a bimetallic chip, *J. Korean Phys. Soc.*, **69**, 793-797 (2016).
26. S. H. Kim, T. U. Kim, H. Y. Jung, H. C. Ki, D. G. Kim, and B.-T. Lee, The effect of Au/Ag bimetallic thin-films on surface plasmon resonance properties comparing with those of Au and Ag single thin-films, *J. Nanosci. Nanotechnol.*, **18**, 1777-1781 (2018).
27. J. M. Fowler, M. C. Stuart, and D. K. Y. Wong, Self-assembled layer of thiolated protein G as an immunosensor scaffold, *Anal. Chem.*, **79**, 350-354 (2007).
28. S. Ghose, M. Allen, B. Hubbard, C. Brooks, and S. M. Cramer, Antibody variable region interactions with protein A: Implications for the development of generic purification processes, *Biotechnol. Bioeng.*, **92**, 666-673 (2005).
29. P. B. Johnson and R. W. Christy, Optical constants of the noble metals, *Phys. Rev. B*, **6**, 4370-4379 (1972).
30. R. Guider, D. Gandolfi, T. Chalyan, L. Pasquardini, A. Samusenko, C. Pederzolli, G. Pucker, and L. Pavesi, Sensitivity and limit of detection of biosensors based on ring resonators, *Sens. Biosensing Res.*, **6**, 99-102 (2015).
31. M. A. Carvajal, J. Ballesta-Claver, A. Martínez-Olmos L. F. Capitán-Vallvey, and A. J. Palma, Portable system for photodiode-based electrochemiluminescence measurement with improved limit of detection, *Sens. Actuators B*, **221**, 956-961 (2015).